Activating Mutations of N-WASP Alter *Shigella* Pathogenesis

David A. Adamovich[1], **Fumihiko Nakamura**[2,3], **Austen Worth**[4], **Siobhan Burns**[4], **Adrian J. Thrasher**[4], **John H. Hartwig**[2,3], and **Scott B. Snapper**[1,2,5]

1 *Gastrointestinal Unit, Massachusetts General Hospital, Boston, MA*

2 *Departments of Medicine, Harvard Medical School*

3 *Hematology Division, Brigham & Women's Hospital*

4 *Molecular Immunology Unit, Institute of Child Health, University College London*

Abstract

The pathogenesis of *Shigella* requires binding to the host protein NWASP. To examine the roles of structural conformation and phospho-regulation of NWASP during *Shigella* pathogenesis, mutant NWASP constructs predicted to result in a constitutively open conformation (L229P and L232P) or either a phospho-mimicking (Y253E) or phospho-disruptive (Y253F) structure were constructed. Pyrene actin assays demonstrated that the NWASP L229P and L232P constructs are constitutively active. Despite the increase in actin polymerization seen *in vitro*, cell lines expressing NWASP L229P and L232P supported shorter actin tails when infected with *Shigella*. *Shigella* actin tails were unchanged in cells expressing NWASP phospho-regulation mutant proteins. *Shigella* invasion, intracellular, and intercellular motility were not altered in cells expressing NWASP L229P or L232P. However, plaque numbers were increased in cells expressing NWASP L229P and L232P. These data demonstrate that NWASP structural conformation is an important regulator of *Shigella* pathogenesis in distinct segments of its lifecycle.

Introduction

Shigella flexneri is a bacterial pathogen of the human intestine that usurps control of the actin cytoskeletal machinery for its pathogenesis [1]. Intracellular *Shigella* movement is facilitated by directing host cell actin polymerization exclusively at one pole of the bacteria - a process known as actin based motility [1]. The force generated by the polymerizing actin is sufficient to propel *Shigella* through the cytoplasm and into neighboring cells [1].

Shigella regulates the host actin cytoskeleton through its interactions with the host protein NWASP [1]. NWASP is a member of the WASP family of cytoskeletal regulators, which interact with various signaling molecules to transduce Arp2/3-mediated actin polymerization [2]. In its native conformation, intramolecular forces hold WASP and NWASP in an auto-inhibited closed, hairpin-like structure [3,4]. Binding of activated Cdc42 to NWASP disrupts this closed conformation, presumably opening up the molecule with a release of auto-inhibition, permitting binding to the Arp2/3 complex and inducing actin polymerization [2]. Once in an open conformation, NWASP can also be modulated by phospho-regulation.

Phosphorylation of tyrosine residue Y253 of NWASP leads to enhanced actin polymerization activity *in vivo* and *in vitro* [5].

Steps controlling activation and regulation of NWASP following *Shigella* IcsA binding are largely unknown. Cdc42 is not absolutely required for *Shigella*-mediated actin-based motility [6]. The role of IcsA and other bacterial/host molecules in the relief of NWASP auto-inhibition is largely unknown. Moreover, the role of phospho-regulation of NWASP during *Shigella*-mediated actin-based motility remains controversial. An early study failed to observe phosphorylated tyrosine residues located at the site of *Shigella*-mediated actin polymerization [7]. However, recent data suggests that the phosphorylation status of NWASP may play an important role in the ability of *Shigella* to form actin tails [8].

Here, we sought to assess the role of NWASP regulation through structural conformation or phosphorylation on *Shigella*-mediated actin-based motility by generating specific mutations in NWASP predicted to regulate structural conformation and phosphorylation, and assessing their behavior during infection.

Materials and Methods

Bacterial strains and cell culture

Shigella flexneri serotype 2a strain 2457T was used for all studies and grown on tryptic soy broth (TSB) with agar containing Congo red as described [17]. Individual red colonies were grown overnight in liquid TSB and then diluted and grown in fresh media until mid-log phase on the day of infection. NWASP$^{-/-}$ mouse embryonic fibroblasts [17] were maintained in Dulbecco's modified Eagle medium (DMEM), supplemented with 10% bovine calf serum (with iron supplement) and L-glutamine.

Generation of NWASP mutations

Point mutations in rat NWASP were generated using an overlapping PCR strategy with WT rate NWASP as a template. The FLAG peptide DNA sequence (5′-atggactacaaggacgacgatgacaag-3′) was inserted before the stop codon at the C-terminal end of NWASP. All constructs were sequenced to verify presence of single point mutations.

Actin polymerization assay

Pyrene actin assays were performed as previously described [23]. Pyrene actin, Cdc42, and the Arp2/3 complex were purified and Cdc42 was loaded with GTPγS. Assays were performed by adding 2uM pyrene actin to a protein mixture of 22.4nM Arp2/3 complex, 500nM Cdc42 GTPγS, and 100nM NWASP. For 20min the fluorescence change was measured at 386 nm with excitation at 366 nm using a luminescence spectrometer (LS50B, Perkin Elmer Life Sciences).

Actin tail length assay

Exponential phase bacteria were centrifuged at 1000 rpm for 15min onto a semi-confluent monolayer of cells seeded on a 20×20mm glass coverslip at an MOI of 100. Cells were incubated for 30 min at 37°C with 5% CO_2. Cells were washed three times with PBS, and then incubated for 2 hours in media containing 50μg/ml gentamicin. Cells were washed 3 times with PBS, then fixed with 3.7% paraformaldehyde in PBS for 10min and stored in 1% BSA in PBS. Following staining, images of 10 different cells per condition per experiment were taken and tail lengths were measured using ImageJ software (Open Source Software). Statistics were performed using the Mann-Whitney Test.

Immunoflorescence microscopy

Fixed cells were permeabilized with 0.2% Triton X-100 in PBS for 5min and washed three times with 1% BSA in PBS. NWASP was stained with mouse αFLAG antibody (SIGMA catalog #F1804) at 1:1000 for 1h, followed by either FITC-conjugated or Cy3-conjugated donkey anti-mouse antibody at 1:200 for 1h. F-actin was stained with rhodamine-labeled or FITC-conjugated phalloidin (1μg/ml in 1% BSA in PBS; Molecular Probes) for 1h. DNA was stained with DAPI (300nM; Molecular Probes) for 10min.

Intracellular motility assay

Exponential phase bacteria expressing GFP were centrifuged at 1000 rpm for 15min onto a semi-confluent monolayer of cells seeded on a glass-bottom 35mm dish at an MOI of 100. Cells were incubated for 30min at 37°C with 5% CO_2. Cells were washed three times with PBS, and incubated in media containing 50μg/ml gentamicin. After 1h, the cells were imaged on a microscope (IX-70; Olympus Optical) with an automated stage using a 100x objective. Images were taken in both the phase and GFP channels every 10s for 15 min. Using Slidebook software (Intelligent Imaging Innovations, Denver, CO), the GFP channel was analyzed to track bacterial movement. Only bacteria moving in at least 10 consecutive frames were counted.

Shigella invasion

Exponential phase bacteria were centrifuged at 1000 rpm for 15 min onto a semi-confluent monolayer of cells seeded on a 20×20mm glass coverslip at an MOI of 100. Cells were incubated for 60min at 37°C with 5% CO_2. Cells were washed 3 times with PBS, then fixed with 3.7% paraformaldehyde in PBS for 10min and stored in 1% BSA in PBS. Cells were stained as described above, and counted microscopically (AX-70; Olympus Optical). Invasion rate is calculated as the number of cells containing internalized bacteria divided by the total number of cells counted multiplied by 100. 100 cells from two different coverslips were counted for each experiment.

Results

Point mutations in NWASP predicted to alter either structural conformation or phospho-regulation result in constitutive activation

A series of point mutations were generated that were predicted to alter either NWASP structural conformation or phospho-regulation (Fig. 1A). A leucine to proline mutation in the homolog human WASP (L270P) leads to a change in the structure of WASP resulting in its open conformation and constitutive activation [9]. We predicted that a homologous mutation in NWASP (L232P) would also lead to a constitutively open and active conformation given the conserved location in the α-helix (Fig. 1A). Similarly, we predicted that a L229P mutation in NWASP, located ~1 turn away from L232 in the critical α-helix, would lead to a constitutively open and active conformation of NWASP (Fig. 1A). Point mutations in NWASP that alter the phospho-regulation of NWASP and cytoskeletal processes have previously been described by Suetsugu *et al.* [5]. We generated both the phospho-mimicking tyrosine to glutamic acid (Y253E) and the phospho-disruptive tyrosine to phenylalanine (Y253F) mutations in NWASP (Fig. 1A).

To assess whether the NWASP L229P and L232P mutations alter baseline actin polymerization activity, we employed a pyrene actin assay. Wild type (WT) NWASP when combined with Arp2/3 and pyrene actin does not lead to significant actin polymerization (Fig. 1B) [10]. However, when activated Cdc42 is added to NWASP, Arp2/3 and pyrene actin, a significant increase in actin polymerization was observed (Fig. 1B). NWASP L229P and L232P, in the

absence of activated Cdc42, polymerizes actin at rates similar or greater than polymerization rates achieved with WT NWASP in the presence of activated Cdc42 (Fig. 1B). Moreover, this constitutive activation of NWASP L229P and NWASP L232P can be further increased by the addition of activated Cdc42 (Fig. 1B). Similar results demonstrating constitutive activation of L229P and L232P were also obtained employing a modified bead assay (Supplementary Fig. 1) [11].

The pyrene actin assay was also employed to assess the activity of the NWASP constructs containing phospho-regulatory mutations. Similar to results obtained with an *in vitro* bead assay using WASP Y291E [12], the homologous NWASP Y253E exhibited an enhanced basal level of actin polymerization compared to WT NWASP (Fig. 1C). This enhanced basal level of activation of NWASP Y253E was also sensitive to Cdc42 stimulation (Fig. 1C). In contrast, the phospho-disruptive NWASP Y253F does not exhibit an enhanced level of actin polymerization compared to WT NWASP, but was sensitive to stimulation by activated Cdc42 (Fig. 1C).

NWASP-deficient cell lines expressing NWASP activation mutations have enhanced migration

To assess, in vivo, the role of each of the NWASP structural conformation and phospho-regulation mutants on a processes that requires dynamic modulation of the actin cytoskeleton (e.g., cell motility), we generated stable cell lines where each mutant construct, or WT NWASP, was expressed in NWASP-deficient cells. The effect of each of the constructs on cell motility was determined employing a standard scratch assay. Cell lines expressing each of the structural conformation and phospho-regulation mutants closed wounds faster than the control cell line expressing WT NWASP (Supplemental Fig 2 and Fig. 1D).

Shigella-mediated actin tail formation does not absolutely require regulation of NWASP structural conformation or phospho-regulation

To assess *Shigella*'s ability to utilize each of the mutant NWASP constructs for actin-based motility, *Shigella* infections were performed in NWASP deficient cell lines that stably expressed each of the NWASP mutants. Each cell line permitted bacterial invasion and supported *Shigella*-mediated actin tail formation, with NWASP localizing appropriately to a bacterial pole (Fig. 2A).

We measured the length of actin tails in *Shigella*-infected cells expressing each of the various NWASP mutants to determine the efficiency by which *Shigella* utilized the NWASP constructs. Tail lengths in *Shigella*-infected NWASP-deficient cells expressing either the phospho-disrupting or phospho-mimicking NWASP mutations (Y253F and Y253E respectively) were similar to those found in cells expressing WT NWASP (Fig. 2B). Using a transient transfection model, the bovine phospho-regulatory mutations described by Suetsugu *et al.* [5] (Y256E/Y256F) were also tested and yielded results similar to those described in Fig. 2B (data not shown). These data demonstrate that the phosphorylation status of Y253 is neither required for nor alters the efficiency of *Shigella*-mediated actin tail formation.

In contrast to the phospho-regulating NWASP mutants, the constitutively active mutants, NWASP L229P and L232P, resulted in subtle yet significantly shorter *Shigella*-mediated tails in stably transfected NWASP-deficient cells (Fig. 2C). Similar results were found when analogous NWASP mutants containing N-terminal GFP fusions were used in transient transfection assays (data not shown). Since the NWASP L229P and L232P mutations are predicted to be in a constitutively open conformation, this implies that while the ability of NWASP to form a closed conformation is not absolutely essential for *Shigella*-mediated actin-

based motility, expression of an activated NWASP molecule is associated with shorter actin tails.

In bacterially infected cells, actin tail length is proportional to the rate of actin polymerization and intracellular speed [13]. We determined the intracellular speed of *Shigella* in cell lines expressing the NWASP mutants employing time-lapse microscopy. In contrast to what may have been predicted based on the modest reduction in actin tail size, intracellular speed was not decreased in NWASP deficient cells expressing the L229P and L232P mutant forms of NWASP compared to WT NWASP (Fig. 2D); indeed, there was a trend towards increased speed in cells expressing the activated molecules.

Shigella plaque numbers are increased in cells expressing constitutively active NWASP

The intercellular spread of *Shigella* is absolutely dependant upon actin based motility [14] and is traditionally assessed by standard plaque assays. Since the NWASP mutant stable cell lines were not conducive to traditional plaque assays, we developed a modified spreading assay (Supplemental Fig 3). An NWASP deficient cell monolayer expressing each of the NWASP constructs was infected with GFP-expressing *Shigella* and assayed after 48 hours to measure intercellular spread. Compared with traditional techniques, this technique facilitated the analysis of a significantly greater number of plaques per experiment.

As shown in Fig. 3A, there were significantly more plaques in the cell lines expressing NWASP L229P ($p < 0.005$) and L232P ($p < 0.0001$) compared to the control cell line expressing WT NWASP. An increase in bacterial invasion was not responsible for the increased number of plaques in cells expressing mutant NWASP L229P and L232P since there was no increase in invasion in cells expressing either of the activated NWASP mutants when compared with WT NWASP (Fig. 3B). In fact, there was a modest decrease in the invasion efficiency in cells expressing the activated mutants that reached statistical significance for NWASP L232P (Fig. 3B; $p = 0.03$). However, despite the increase in the number of plaques, there was no difference in the diameter of plaques formed in the cell lines expressing L229P and L232P compared to the cell line expressing WT NWASP (Fig. 3C), indicating that the rate of intercellular spread is not altered by expression of activated NWASP.

Discussion

Intracellular pathogens exploit diverse mechanisms to modulate the host actin cytoskeleton during infection [1]. *Shigella* IcsA binds and activates host-encoded NWASP resulting in activation of Arp-2/3 dependent actin assembly [15,16]. The processes that regulate NWASP activation during *Shigella* infection are largely unknown. We have examined whether the actin-based motility of *Shigella* requires active modulation of the structure and phosphorylation of NWASP during infection.

We demonstrate that NWASP L232P mutation, homologous to the WASP L270P mutation implicated in X-linked neutropenia [9], results in the constitutive activation of NWASP. In addition, a proline mutation in a neighboring leucine residue can also lead to constitutive NWASP activation. These studies reproduce previously published results demonstrating that the NWASP Y253E mutation has an enhanced intrinsic actin polymerization activity compared to WT NWASP, and that the NWASP Y253F mutation behaves similar to WT NWASP in the pyrene actin assay [5]. Activation by the structural conformation (L229P and L232P) and phospho-mimicking (Y253E) NWASP mutations could be further enhanced *in vitro* by the addition of Cdc42 – suggesting that these mutations may not result in complete disruption of auto-inhibition *in vivo*.

We have demonstrated that *Shigella*-mediated actin assembly occurs independent of NWASP phosphorylation at Y253 – a site previously shown to be required for modulation of the actin cytoskeleton during neurite extension [5]. Moreover, the efficiency of actin tail formation does not seem to require this form of phospho-regulation since tail lengths were similar in cells expressing WT NWASP or either the phospho-mimicking (Y253E) or phospho-disruptive (Y253F) NWASP. This work contrasts with another study that showed that phosphorylation of Y253 in NWASP regulates the length of *Shigella*-induced actin tails [8]. Shorter actin tails were observed upon *Shigella* infection when a phospho-disruptive NWASP Y253F mutant was expressed in NWASP deficient cells employing transient transfection techniques [8]. In these studies, inhibition of tyrosine phosphorylation using the Abl/Arg kinase inhibitor Gleevac also inhibited tail length [8]. We observed no affect of the phospho-disruptive mutation on *Shigella*-mediated actin assembly employing either stable cell lines (Fig. 3B) or in transient transfection assays (data not shown). Moreover, Gleevac had no affect on *Shigella*-mediated actin tail formation in our studies (data not shown). Although we have no obvious explanation for the differences in results obtained in each of these studies – the NWASP-deficient cell lines in each of the studies were obtained from different mouse lines [17,18].

Our data indicate that a constitutively active NWASP mutant protein can readily support *Shigella*-mediated actin assembly and movement. In contrast to bacterial speed, the size of *Shigella* tails was modestly reduced in cells expressing constitutively active NWASP L299P or L232P as compared to cells expressing WT NWASP. Leung *et al.* did not observe a difference in *Shigella*-mediated actin tails in NWASP deficient cells expressing human NWASP L235P (homologous to NWASP L232P) compared to cells expressing WT human NWASP [19]. Given the shorter tail lengths without concomitant reductions in bacterial speed associated with these mutations, our data is consistent with a model by which activated NWASP results in an increase in actin polymerization yet may have a more pronounced direct or indirect role on actin depolymerization [20]. Our data showing that NWASP L229P or L232 led to increased actin polymerization and increased migration of cells in vitro gives support to this model.

The increased number of plaques formed in the cell monolayers expressing NWASP L229P and L232P as compared to those expressing WT NWASP suggests that a change in the activation of NWASP through modulation of its resting conformation alters *Shigella* pathogenesis. An altered rate of bacterial invasion could not explain the differences in plaque numbers since the rate of bacterial invasion was similar among the different cell lines (Fig. 3B). Moreover, mechanisms that enhance the rate of intercellular spreading could not explain the observation of increased plaque numbers because there was no difference in the diameter of the plaques formed in each of the cell lines (Fig. 3C). An increase in plaque numbers may reflect an alteration in the rate by which *Shigella* is cleared following invasion from the extracellular environment when an activated NWASP is present in host cells. In this regard, *Shigella* uptake into autophagosomes has been shown to be dependent upon the presence of IcsA [21] and the process of autophagy is dependent upon Arp2/3 activation [22].

Supplementary Material

Refer to Web version on PubMed Central for supplementary material.

References

1. Gouin E, Welch MD, Cossart P. Actin-based motility of intracellular pathogens. Curr Opin Microbiol 2005;8:35–45. [PubMed: 15694855]

2. Takenawa T, Suetsugu S. The WASP-WAVE protein network: connecting the membrane to the cytoskeleton. Nat Rev Mol Cell Biol 2007;8:37–48. [PubMed: 17183359]

3. Miki H, Takenawa T. Direct binding of the verprolin-homology domain in N-WASP to actin is essential for cytoskeletal reorganization. Biochem Biophys Res Commun 1998;243:73–78. [PubMed: 9473482]

4. Kim AS, Kakalis LT, Abdul-Manan N, Liu GA, Rosen MK. Autoinhibition and activation mechanisms of the Wiskott-Aldrich syndrome protein. Nature 2000;404:151–158. [PubMed: 10724160]

5. Suetsugu S, Hattori M, Miki H, Tezuka T, Yamamoto T, Mikoshiba K, Takenawa T. Sustained activation of N-WASP through phosphorylation is essential for neurite extension. Dev Cell 2002;3:645–658. [PubMed: 12431372]

6. Shibata T, Takeshima F, Chen F, Alt FW, Snapper SB. Cdc42 facilitates invasion but not the actin-based motility of Shigella. Curr Biol 2002;12:341–345. [PubMed: 11864577]

7. Frischknecht F, Moreau V, Rottger S, Gonfloni S, Reckmann I, Superti-Furga G, Way M. Actin-based motility of vaccinia virus mimics receptor tyrosine kinase signalling. Nature 1999;401:926–929. [PubMed: 10553910]

8. Burton EA, Oliver TN, Pendergast AM. Abl kinases regulate actin comet tail elongation via an N-WASP-dependent pathway. Mol Cell Biol 2005;25:8834–8843. [PubMed: 16199863]

9. Devriendt K, Kim AS, Mathijs G, Frints SG, Schwartz M, Van Den Oord JJ, Verhoef GE, Boogaerts MA, Fryns JP, You D, Rosen MK, Vandenberghe P. Constitutively activating mutation in WASP causes X-linked severe congenital neutropenia. Nat Genet 2001;27:313–317. [PubMed: 11242115]

10. Ho HY, Rohatgi R, Lebensohn AM, Kirschner MW. In vitro reconstitution of cdc42-mediated actin assembly using purified components. Methods Enzymol 2006;406:174–190. [PubMed: 16472658]

11. Ancliff PJ, Blundell MP, Cory GO, Calle Y, Worth A, Kempski H, Burns S, Jones GE, Sinclair J, Kinnon C, Hann IM, Gale RE, Linch DC, Thrasher AJ. Two novel activating mutations in the Wiskott-Aldrich syndrome protein result in congenital neutropenia. Blood 2006;108:2182–2189. [PubMed: 16804117]

12. Cory GO, Garg R, Cramer R, Ridley AJ. Phosphorylation of tyrosine 291 enhances the ability of WASp to stimulate actin polymerization and filopodium formation. Wiskott-Aldrich Syndrome protein. J Biol Chem 2002;277:45115–45121. [PubMed: 12235133]

13. Theriot JA, Mitchison TJ, Tilney LG, Portnoy DA. The rate of actin-based motility of intracellular Listeria monocytogenes equals the rate of actin polymerization. Nature 1992;357:257–260. [PubMed: 1589024]

14. Makino S, Sasakawa C, Kamata K, Kurata T, Yoshikawa M. A genetic determinant required for continuous reinfection of adjacent cells on large plasmid in S. flexneri 2a. Cell 1986;46:551–555. [PubMed: 3524856]

15. Egile C, Loisel TP, Laurent V, Li R, Pantaloni D, Sansonetti PJ, Carlier MF. Activation of the CDC42 effector N-WASP by the Shigella flexneri IcsA protein promotes actin nucleation by Arp2/3 complex and bacterial actin-based motility. J Cell Biol 1999;146:1319–1332. [PubMed: 10491394]

16. Suzuki T, Miki H, Takenawa T, Sasakawa C. Neural Wiskott-Aldrich syndrome protein is implicated in the actin-based motility of Shigella flexneri. Embo J 1998;17:2767–2776. [PubMed: 9582270]

17. Snapper SB, Takeshima F, Anton I, Liu CH, Thomas SM, Nguyen D, Dudley D, Fraser H, Purich D, Lopez-Ilasaca M, Klein C, Davidson L, Bronson R, Mulligan RC, Southwick F, Geha R, Goldberg MB, Rosen FS, Hartwig JH, Alt FW. N-WASP deficiency reveals distinct pathways for cell surface projections and microbial actin-based motility. Nat Cell Biol 2001;3:897–904. [PubMed: 11584271]

18. Lommel S, Benesch S, Rottner K, Franz T, Wehland J, Kuhn R. Actin pedestal formation by enteropathogenic Escherichia coli and intracellular motility of Shigella flexneri are abolished in N-WASP-defective cells. EMBO Rep 2001;2:850–857. [PubMed: 11559594]

19. Leung Y, Ally S, Goldberg MB. Bacterial actin assembly requires toca-1 to relieve N-wasp autoinhibition. Cell Host Microbe 2008;3:39–47. [PubMed: 18191793]

20. Carlier MF, Laurent V, Santolini J, Melki R, Didry D, Xia GX, Hong Y, Chua NH, Pantaloni D. Actin depolymerizing factor (ADF/cofilin) enhances the rate of filament turnover: implication in actin-based motility. J Cell Biol 1997;136:1307–1322. [PubMed: 9087445]

21. Ogawa M, Yoshimori T, Suzuki T, Sagara H, Mizushima N, Sasakawa C. Escape of intracellular Shigella from autophagy. Science 2005;307:727–731. [PubMed: 15576571]

22. Monastyrska I, He C, Geng J, Hoppe AD, Li Z, Klionsky DJ. Arp2 links Autophagic Machinery with the Actin Cytoskeleton. Mol Biol Cell. 2008

23. Blanchoin L, Amann KJ, Higgs HN, Marchand JB, Kaiser DA, Pollard TD. Direct observation of dendritic actin filament networks nucleated by Arp2/3 complex and WASP/Scar proteins. Nature 2000;404:1007–1011. [PubMed: 10801131]
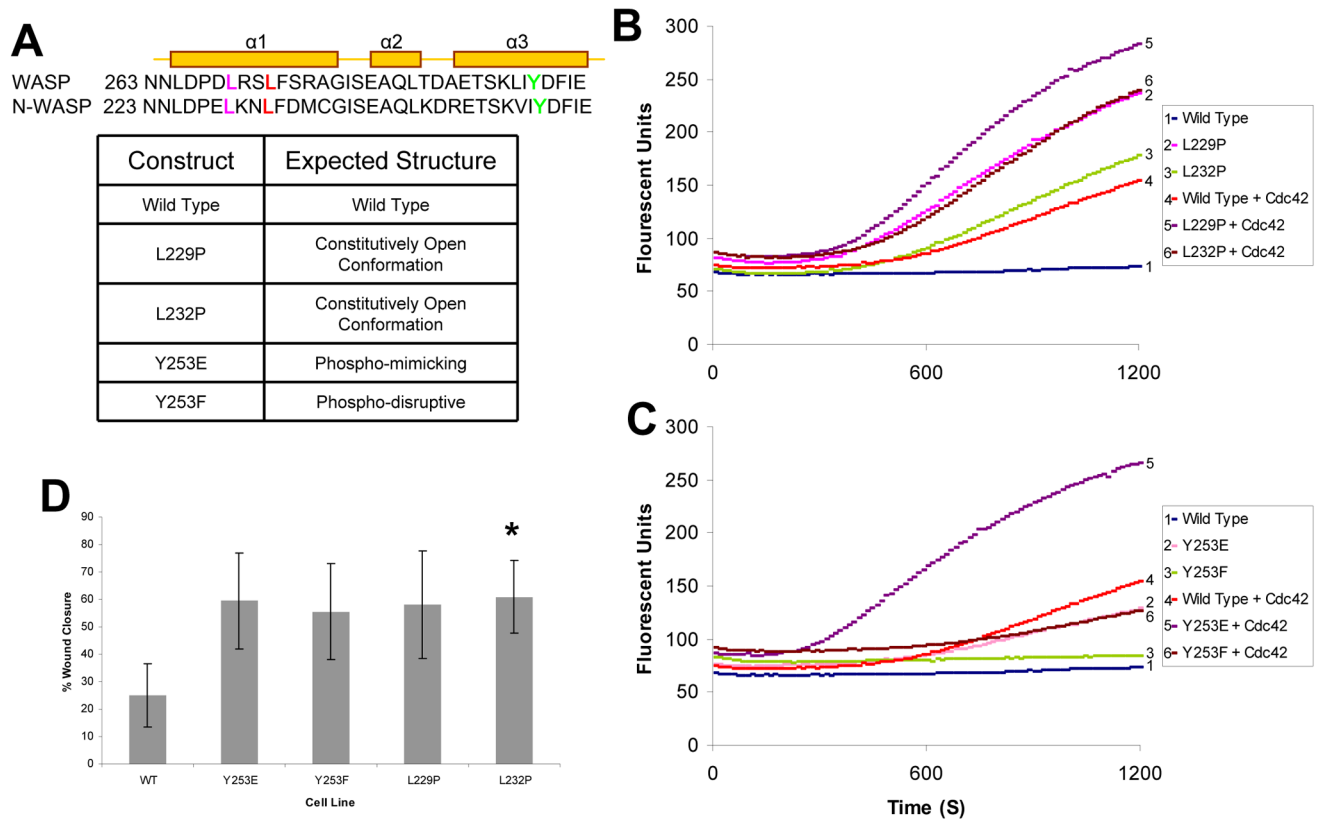
Fig. 1. NWASP mutations result in constitutive activation
(A) Protein sequence alignment of a portion of the GBD of murine WASP and rat NWASP. Predicted tertiary structure of the sequence denoting α-helixes is shown [4]. The residues selected for mutations are L229 in purple, L232 in red, and Y253 in green. Table represents the predicted structural phenotypes for each of the NWASP mutants. (B) Pyrene actin assay measuring the actin polymerization activity of NWASP mutations predicted to have an open conformation in the presence/absence of Cdc42-GTPγS. (C) Pyrene actin assay with phospho-regulatory NWASP in the presence/absence of Cdc42-GTPγS. (D). Histogram demonstrating that NWASP-deficient fibroblasts expressing NWASP phospho-regulatory (Y253E and Y253F) or constitutively active (L229P & L232P) constructs result in increased migration in a scratch assay (* $p < 0.05$).
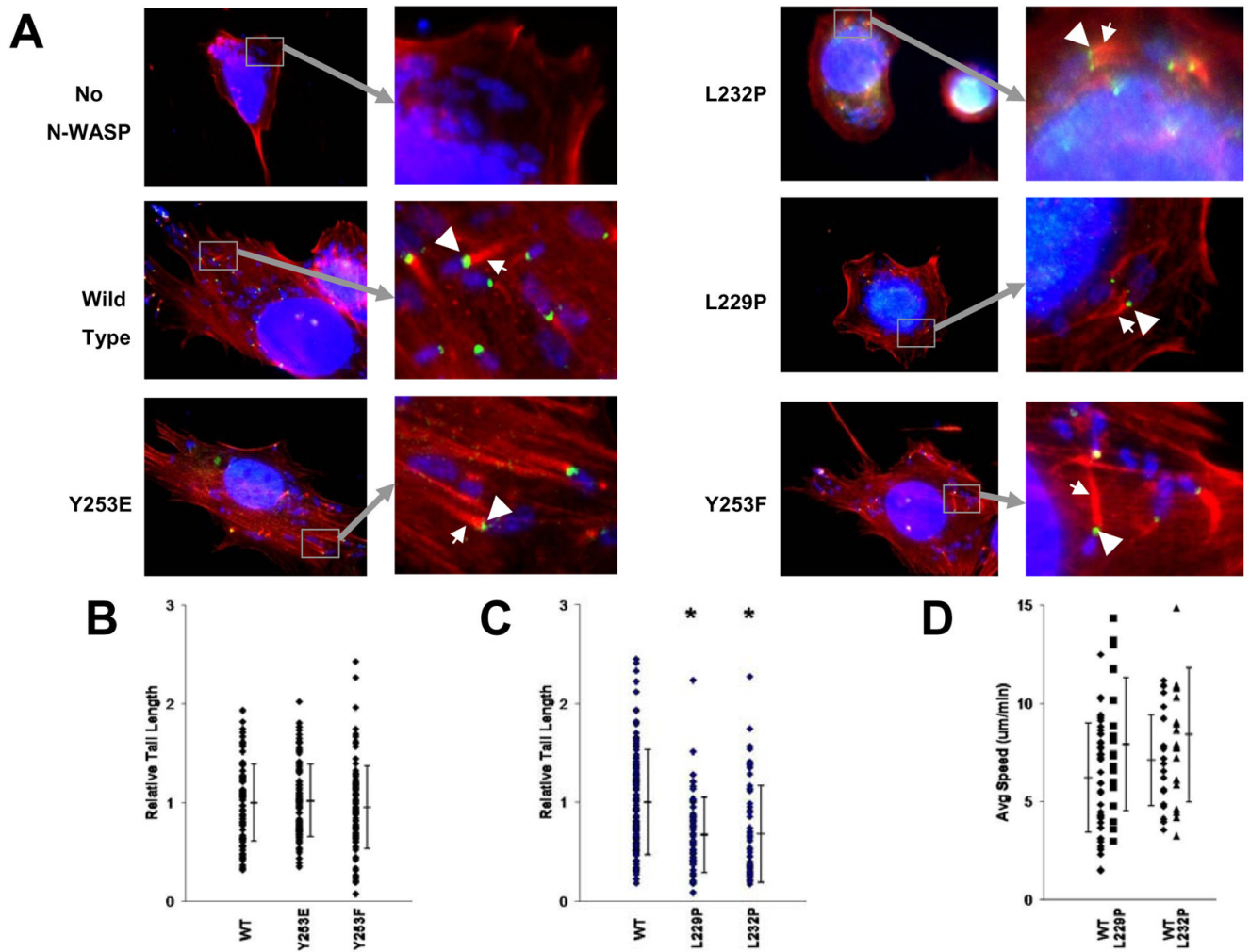
Fig. 2. NWASP regulatory mutants localize appropriately and support *Shigella*-mediated actin based motility

(A) Stable cell lines expressing each of the NWASP constructs were infected with *Shigella*. Cells were stained for DNA (blue), NWASP (green), and actin (red). Insets show polar NWASP localization (arrow heads) and actin tail formation (arrows). (B) Tails formed in cells expressing NWASP Y253E and Y253F are similar in length to those expressed in cells expressing WT NWASP. (C) Tails formed in cells expressing NWASP L229P and L232P are shorter in length than those expressed in cells expressing WT NWASP. * P<.05 (Mann-Whitney test). (D) Time lapse microscopy was used to quantify the velocity of *Shigella* undergoing actin-based motility. Average speed of *Shigella* in cells expressing WT NWASP, L229P, or L232P is shown.
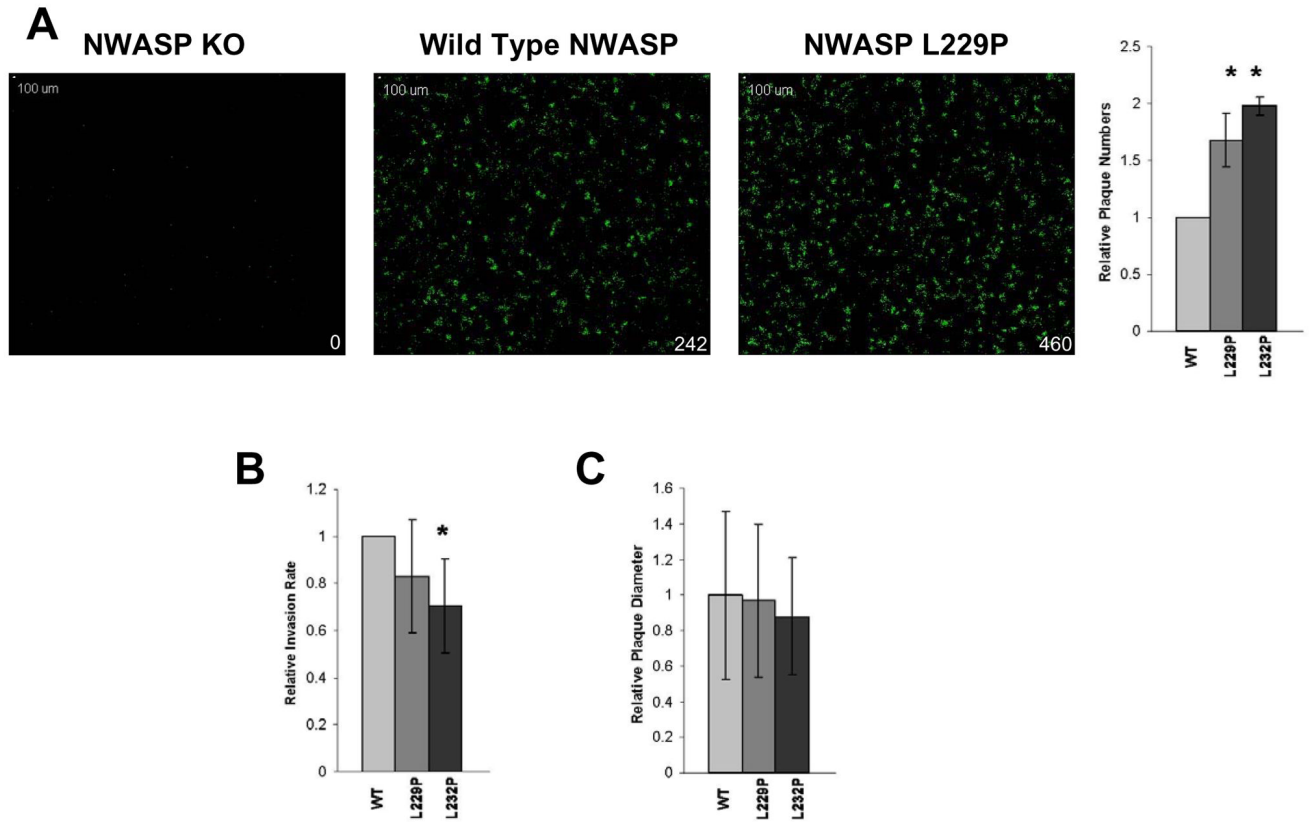
Fig. 3. Markedly increased plaque numbers, but not invasion rate or intercellular spread, in cells expressing constitutively active NWASP

(A) Increased number of plaques formed in cell lines expressing constitutively active NWASP L229 and L2332. Representative monolayers imaged 48h after infection with GFP expressing *Shigella*. Green signal represents *Shigella* plaques (inset indicates number of plaques in monolayer). Histogram on right is quantification of three independent experiments. (B) *Shigella* invasion rates are compared in stable cell lines expressing WT, L229 or L2332 NWASP constructs. Results shown are average of three independent experiments (* $p < 0.05$). (C) The average size of plaques formed in each cell line expressing mutant NWASP constructs was not significantly different from cell lines expressing WT NWASP. Combined results of three individual experiments are shown.